Evolutionary signal of leaflet anatomy in the Zamiaceae

Coiro, Mario ; Jelmini, Nicola ; Neuenschwander, Hanna ; Calonje, Michael A ; Vovides, Andrew P ; Mickle, James E ; Barone Lumaga, Maria Rosaria

Abstract: Premise of research: The morphology of leaves is shaped by both historical and current selection acting on constrained developmental systems. For this reason, the phylogenetic signal of these characters is usually overlooked. Methodology: We investigate morphology of the leaflets of all genera of the Zamiaceae using multiple microscopical techniques to test whether leaf characters present a phylogenetic signal and whether they are useful to define clades at a suprageneric level. Pivotal results: Our investigation shows that most genera are quite uniform in their leaflet anatomy, with the largest genera (Zamia, Encephalartos) presenting the highest degree of variation. Using both Bayesian and parsimony methods on two different molecular scaffolds, we are able to show that leaflet anatomy has a strong phylogenetic signal in the Zamiaceae and that many clades retrieved by molecular analyses present potential synapomorphies in their leaflet anatomy. Particularly, the placement of Stangeria in a clade with Zamia and Microcycas is supported by the presence of both an adaxial and an abaxial girder sclerenchyma and the absence of sclerified hypodermis. The placement of Stangeria as sister to Bowenia, on the other hand, is not supported by our analysis. Instead, our results put into question the homology of the similar guard cell morphology in the two genera. Conclusions: We show that leaflet anatomy has a substantial amount of phylogenetic signal in the Zamiaceae, supporting relationships that are not supported by general morphology. Therefore, anatomical investigation represents a promising avenue for plant systematists.

DOI: https://doi.org/10.1086/709372

Originally published at:
Coiro, Mario; Jelmini, Nicola; Neuenschwander, Hanna; Calonje, Michael A; Vovides, Andrew P; Mickle, James E; Barone Lumaga, Maria Rosaria (2020). Evolutionary signal of leaflet anatomy in the Zamiaceae. International Journal of Plant Sciences, 181(7):697-715.
DOI: https://doi.org/10.1086/709372

Int. J. Plant Sci. 181(7):000–000. 2020.

1058-5893/2020/18107-00XX$15.00 DOI: 10.1086/709372

EVOLUTIONARY SIGNAL OF LEAFLET ANATOMY IN THE ZAMIACEAE

Mario Coiro,[1,]* Nicola Jelmini,* Hanna Neuenschwander,* Michael A. Calonje,† Andrew P. Vovides,‡ James E. Mickle,§ and Maria Rosaria Barone Lumaga‖

*Department of Systematic and Evolutionary Botany, University of Zurich, Zurich, Switzerland; †Department of Biological Sciences, Florida International University, Miami, Florida, USA, and Montgomery Botanical Center, Coral Gables, Florida, USA; ‡Red de Biología Evolutiva, Instituto de Ecología, A.C., Xalapa, Veracruz, Mexico; §Department of Plant and Microbial Biology, North Carolina State University, Raleigh, North Carolina, USA; and ‖Department of Biology, University of Naples Federico II, Naples, Italy

Editor: Stefanie Ickert-Bond

Premise of research. The morphology of leaves is shaped by both historical and current selection acting on constrained developmental systems. For this reason, the phylogenetic signal of these characters is usually overlooked.

Methodology. We investigate morphology of the leaflets of all genera of the Zamiaceae using multiple microscopical techniques to test whether leaf characters present a phylogenetic signal and whether they are useful to define clades at a suprageneric level.

Pivotal results. Our investigation shows that most genera are quite uniform in their leaflet anatomy, with the largest genera (*Zamia*, *Encephalartos*) presenting the highest degree of variation. Using both Bayesian and parsimony methods on two different molecular scaffolds, we are able to show that leaflet anatomy has a strong phylogenetic signal in the Zamiaceae and that many clades retrieved by molecular analyses present potential synapomorphies in their leaflet anatomy. Particularly, the placement of *Stangeria* in a clade with *Zamia* and *Microcycas* is supported by the presence of both an adaxial and an abaxial girder sclerenchyma and the absence of sclerified hypodermis. The placement of *Stangeria* as sister to *Bowenia*, on the other hand, is not supported by our analysis. Instead, our results put into question the homology of the similar guard cell morphology in the two genera.

Conclusions. We show that leaflet anatomy has a substantial amount of phylogenetic signal in the Zamiaceae, supporting relationships that are not supported by general morphology. Therefore, anatomical investigation represents a promising avenue for plant systematists.

Keywords: Cycadales, morphology, xeromorphy, convergence, paedomorphosis.

Online enhancements: supplementary figures and tables.

Introduction

Cycads represent an extremely charismatic group for both scientists and laypeople. Among seed plants, they are supposed to retain many plesiomorphic characters (Brenner et al. 2003). This, together with the (often superficial) resemblance of leaves of extant cycads to the relatively rare fossils of presumed Mesozoic relatives, has built their reputation as "living fossils." Our modern understanding of the group paints a more dynamic picture: if some of the extant genera seem to have a deep history (Coiro and Pott 2017), most of the species diversity within genera seems to have originated much more recently than the presumed Mesozoic peak of disparity (Harris 1961), potentially postdating the mid-Miocene climate change (Nagalingum et al. 2011; Condamine et al. 2015).

The systematics of Cycadales, which currently includes 10 genera, has traditionally seen the genus *Cycas* L. clearly segregated from the rest of the order and belonging to its own family, Cycadaceae. However, the relationships of some of the more morphologically distinct genera, that is, *Bowenia* Hook. and *Stangeria* T.Moore, with respect to the more "canonical" Zamiaceae have proven to be more problematic (fig. 1). Johnson (1959) segregated *Stangeria* into its own family, Stangeriaceae, including *Bowenia* within Zamiaceae. Stevenson (1981) subsequently separated the latter genus into its own family, Boweniaceae, on the basis of the presence of a unique circinate pinna ptyxis. With the introduction of a formal phylogenetic analysis based on morphology, Stevenson (1990) retrieved a sister relationship between *Bowenia* and *Stangeria*. He later included both genera within his circumscription of Stangeriaceae, which was placed as sister to the Zamiaceae (Stevenson 1992). Stevenson

[1] Author for correspondence; email: mario.coiro@systbot.uzh.ch.

Manuscript received November 2019; revised manuscript received January 2020; electronically published August 7, 2020.

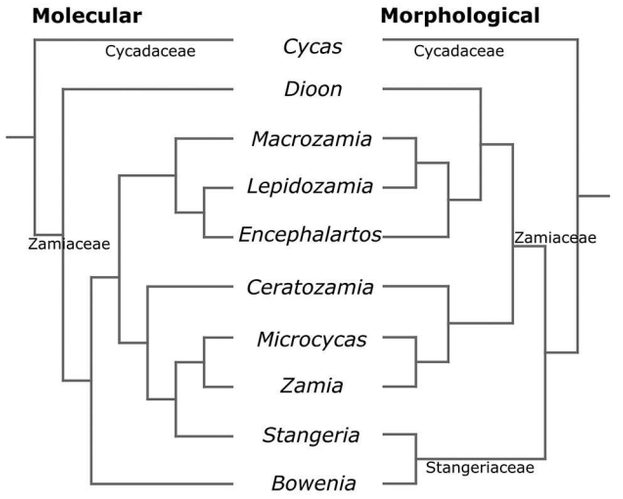

Fig. 1 Comparison of some of the relationships among cycads inferred using molecular and morphological data. The tree on the left represents the relationships found in Salas-Leiva et al. (2013), while the tree on the right represents the relationships found in Stevenson (1990).

(1992) also introduced subfamilial groups within Zamiaceae, with the Encephalartoideae including *Dioon* Lindl., *Encephalartos* Lehm., *Lepidozamia* Regel, and *Macrozamia* Miq. and the Zamioideae including *Ceratozamia* Brongn., *Microcycas* A.DC., *Zamia* L., and *Chigua* D.W.Stev., the latter of which has now been subsumed into *Zamia* (Lindstrom 2009).

Stevenson's morphology-based familial classification has been challenged by strong molecular evidence showing that the members of Stangeriaceae (*Stangeria* and *Bowenia*) are nested within Zamiaceae (Rai et al. 2003; Zgurski et al. 2008; Salas-Leiva et al. 2013). Moreover, the subfamilial classification of Stevenson (1992) also appears to be at odds with the molecular evidence: *Dioon* is consistently retrieved as sister to all other Zamiaceae; *Encephalartos*, *Lepidozamia*, and *Macrozamia* form a strongly supported clade, with *Lepidozamia* sister to *Encephalartos*; and the Zamioideae appear to be paraphyletic, with *Stangeria* nested within them as sister either to *Ceratozamia* (Nagalingum et al. 2011) or to *Microcycas* plus *Zamia* (Salas-Leiva et al. 2013). The placement of *Bowenia* is more uncertain; it is placed as sister to all Zamiaceae except for *Dioon* (Salas-Leiva et al. 2013), sister to the *Macrozamia-Encephalartos-Lepidozamia* clade, or sister to the *Ceratozamia-Stangeria-Microcycas-Zamia* clade (*PHYP* matrix of Nagalingum et al. 2011). The inconsistent topologies revealed in different phylogenetic studies have led to the reinclusion of *Bowenia* and *Stangeria* in Zamiaceae (Christenhusz et al. 2011).

The results from the molecular studies conflict with the phylogenies suggested by morphology and open the possibility of convergent patterns masking the phylogenetic signal of morphology. In plants, both vegetative and reproductive traits can present high degrees of convergence: reproductive structures tend to converge on similar morphologies because of selection on pollination mode (Fenster et al. 2004), while leaves and other vegetative organs tend to vary with the environment of the species in a similar, predictable way (Wright et al. 2004; Gutiérrez-Ortega et al. [2018] for the cycad genus *Dioon*). In spite of these well-known patterns, morphology can still present a surprising degree of phylogenetic signal in plants (Coiro et al. 2018).

Many of the first anatomical studies of cycad leaflets were undertaken in order to advance the understanding of the relationship between fossil and extant taxa, with many authors focusing on cuticular characters that can be retrieved in fossils (Thomas and Bancroft 1913; Florin 1933; Greguss 1968). Only a few authors stressed the importance of other aspects of the anatomy of the leaflets (e.g., Lamb 1923; Stevenson et al. 1996). Recently, a revival of the studies on leaflet anatomy has shown it to be a good source of characters to distinguish among species (Pérez-Farrera et al. 2014) and has recovered a high level of uniformity in leaflet anatomy within genera, that is, in *Cycas* (Griffith et al. 2014) and in *Dioon* (Barone Lumaga et al. 2015; Magellan et al. 2018; Vovides et al. 2018). However, little attention has been paid to the systematic value of leaflet anatomy at the suprageneric level.

Here, we conduct an investigation of leaflet anatomical characters across Zamiaceae, including all nine genera, employing traditional anatomical techniques as well as new techniques such as confocal microscopy. This allowed us to test the presence of variation in leaflet anatomy at both generic and suprageneric levels. We then summarized the information present in the literature and combined this with our observations to test hypotheses of congruence between the relationships supported by molecular data and the distribution of leaflet anatomical characters. In particular, we tested whether leaflet anatomy presents synapomorphies for the major groups in the Zamiaceae and whether it supports the placement of *Stangeria* in the *Ceratozamia-Microcycas-Zamia* clade.

Material and Methods

Sampling

Leaflet samples were collected from plants grown at the Botanical Garden of the University of Naples, Naples, Italy (NAP); the Montgomery Botanical Center in Coral Gables, Florida (MBC); the Botanical Garden of the University of Zurich, Zurich, Switzerland (UZH); the Nong Nooch Botanical Garden, Thailand (NN); the Fairchild Tropical Botanic Garden, Florida (FTBG); the Jardín Botánico Francisco Javier Clavijero, Veracruz, Mexico (JBC); and private collections. We sampled either whole leaflets, when possible, or sections of the median part of the leaflets. All observations were conducted on the median part of the leaflets. We sampled all extant genera of the Zamiaceae, including both species of *Bowenia* and the monotypic *Microcycas* and *Stangeria*, as well as species of *Ceratozamia* (five species sampled), *Dioon* (nine species sampled), *Encephalartos* (11 species sampled), *Lepidozamia* (one species sampled), *Macrozamia* (five species sampled), and *Zamia* (21 species sampled). A full list of the samples is given in table S1 (tables S1–S3 are available online). The literature was also searched for other treatments of cycad leaflet anatomy, and characters were scored on the basis of observation of illustrated sections.

Material Preparation

Samples of leaflets for embedding were cut into ~1-cm^2 pieces using a razor blade, were fixed in formalin–acetic acid–alcohol

(FAA; 10:5:50) overnight, and were then transferred to 70% ethanol for preservation. For observation of external surfaces using SEM, samples were fixed in FAA or in ethanol 50% (the fixation with ethanol reduces costs and the toxicity of the reagents used, producing, at the same time, excellent samples for SEM observation) and then were dehydrated in a graded ethanol series and critical-point dried in liquid CO_2. Cuticles for SEM observation were prepared by treating samples with 20% Cr_2O_3 (Alvin and Boulter 1974) for up to 72 h. Isolated cuticles were then washed several times in distilled water, mounted on aluminum stubs, and air-dried.

Sectioning

Hand sections were cut from leaf samples using a hand microtome. Unstained sections were then transferred into glycerol for imaging and were then transferred into Hoyer's medium (prepared according to Coiro and Truernit [2017]) for permanent mounting. Sections for staining were mounted directly in Hoyer's or mounted in water for imaging (phloroglucinol).

Staining and Histochemistry

Hand sections were stained using pseudo-Schiff propidium idodide (PS-PI) staining according to the protocol of Coiro and Truernit (2017) so that mucilage canals could be identified. Freshly made hand sections were stained using a solution of 0.1 g phloroglucinol (Sigma) in 100 mL 95% ethanol, where 12 mL of concentrated HCl were added. Sections were left to incubate for 15–30 min and then were quickly transferred to glycerol for observation.

Light and Fluorescence Microscopy

All hand-cut sections were observed with a Zeiss Axioscope and photographed with a Zeiss AxioCam HRc with a Zeiss HF bright-field fluorescence filter.

Confocal Microscopy

Processing for confocal microscopy was conducted as previously described in Barone Lumaga et al. (2015). PS-PI–stained samples of *S. eriopus* (Kunze) Baill. and *B. spectabilis* Hook. ex Hook.f. were observed using a Leica TCS SP8 microscope. Excitation was obtained using a 488-nm and 405-nm diode laser.

SEM

All samples for SEM were coated to ca. 25 nm with gold. Specimens were observed under an FEI Quanta 200 ESEM at an accelerating voltage of 25 kV.

Image Analysis

Raw images were analyzed and measured using the software Fiji (Schindelin et al. 2012), with brightness and contrast adjusted using the "auto" option in the software.

Phylogenetic Analysis

To reconstruct the evolution of characters on the phylogeny of the Zamiaceae, we estimated a dated phylogeny of the order Cycadales. We used the molecular matrix of Condamine et al. (2015; including two plastid loci [*matK* and *rbcL*] and one nuclear locus [*PHYP*]). This matrix was trimmed to include only crown group Cycadales and was then polished by the removal of synonymous taxa (per the World List of Cycads), and new sequences for *matK* and *rbcL* were integrated using data from Clugston et al. (2016; listed in table S2) and were aligned with the rest of the sequences by hand. This resulted in an alignment of 228 taxa.

This matrix was then analyzed using BEAST2 as implemented with the CIPRES Science Gateway (Drummond and Rambaut 2007; Suchard and Rambaut 2009; Miller et al. 2010). The input XML file was generated using BEAUTi for BEAST2. The three markers were analyzed under separate site model partitions, while the clock model was linked between the two plastid markers. Site models were averaged for each gene partition using bModelTest (Bouckaert and Drummond 2017). The uncorrelated lognormal relaxed clock was implemented for both clock partitions. A birth-death prior was used for the tree, as it has been demonstrated to be the best prior for the parent data set (Condamine et al. 2015). Four node calibrations were employed, all implemented using uniform distributions. The root of the Cycadales was calibrated with the age of the fossil sporophyll *Crossozamia* (Gao and Thomas 1989) as the minimum age constraint (265.1 mya, middle Permian) and the oldest age for the Carboniferous (358.9 mya) as the maximum age constraint, representing the oldest crown group fossils of the seed plants. The age of *Crossozamia* was also used as a conservative maximum for all other calibrations. The stem group of *Bowenia* was calibrated using the Eocene fossils *B. eocenica* Hill and *B. papillosa* Hill (Hill 1978), with a minimum age of 33.9 mya. The split between *Encephalartos* and *Lepidozamia* was calibrated using the Eocene fossil *L. foveolata* Hill (Hill 1980; minimum age, 33.9 mya). The split between the *Encephalartos-Lepidozamia* clade and *Macrozamia* was calibrated using the fossil *Austrozamia stockeyi* from the Early Eocene Laguna del Hunco locality (Wilf et al. 2016; minimum age, 52 mya). We used this fossil to calibrate this node instead of the stem of Encephalartinae (as suggested by Wilf et al. 2016) because the extreme cuticular similarity between *Encephalartos* and *Lepidozamia* and the divergent morphology of *Macrozamia* (see Coiro and Pott 2017) seem to suggest that *Austrozamia* is closer to the *Encephalartos-Lepidozamia* clade than to *Macrozamia*. The split between *Zamia* and *Microcycas* was calibrated using *Z. nelliae* from the Eocene of Panama (Erdei et al. 2018). All nodes corresponding to dating calibrations were constrained to be monophyletic. For the topology of the tree, two different analyses were run: one with a mostly unconstrained topology (with the exception of the calibrated nodes) and another with *Stangeria* constrained as sister to *Microcycas* and *Zamia* (per Salas-Leiva et al. 2013), the Caribbean *Zamia* as sister to the mainland *Zamia* (per Calonje et al. 2019), and *Dioon* as sister to the other Zamiaceae.

Two separate chains were run for 10,000,000 generations, sampling every five-thousandth generation for each of the two analyses. Convergence was checked by looking at the effective sample size (ESS) of the parameters of the Markov chain Monte Carlo using Tracer (Rambaut et al. 2018), waiting for ESS higher than 200. Tree posteriors were then combined by removing the first 10% as burn-in and subsampling to the one-hundred-thousandth generation using LogCombiner. Maximum clade credibility trees

were obtained using TreeAnnotator as implemented with the CIPRES Science Gateway.

Ancestral State Reconstruction

To reconstruct the evolutionary history of the characters identified here, we employed stochastic character mapping (Bollback 2006). First, we converted the summary table of the traits (table 1) to a comma-separated values format. We then modified character scoring by coding discontinuous adaxial sclerified hypodermis as absent, coding parenchymatous abaxial girder sclerenchyma as simply present, and splitting the palisade parenchyma character into a lobation character (lobed, unlobed, undifferentiated) and a character representing the number of layers (one, two, many). To test the potential homologies of the multiple canals of *Ceratozamia*, we employed alternative coding schemes: in the first, we coded the presence of one large canal between the vascular bundles and multiple smaller canals as separate states (coding 1), while in the second, they were merged into a single state (canals between vascular bundles; coding 2). We then trimmed the trees from the unconstrained and constrained analyses to include only the species with the coded characters. These trees were then used to reconstruct the evolutionary history of all the characters identified using the function make.simmap from the package phytools (Revell 2012). First, the best model for the substitution matrix was selected for each character by obtaining the corrected Akaike information criterion (AICc) using the fitDiscrete function from the package GEIGER (Harmon et al. 2008). One hundred replicates were run using the best model (i.e., with the lowest AICc or, in case of identical AICc, the lowest number of parameters; AICc found in table S3). The two trimmed trees were also used to reconstruct trait evolution using parsimony and to compute both consistency indexes and retention indexes in Mesquite (Maddison and Maddison 2005). λ values for all characters were inferred using the function fitDiscrete from the package GEIGER (Harmon et al. 2008), implementing the best model found for the substitution matrix. We also tested whether the number of parsimony steps observed differed significantly from a random null obtained by randomizing the character state at the tips (Maddison and Slatkin 1991) using a custom script from Bush et al. (2016). The randomization was run for 999 replications.

Results

Anatomical Descriptions

Epidermal pavement cells. The epidermis of the leaflets is usually composed of sclerified thick-walled pavement cells (fig. 2). All genera present cells with thinner walls interspersed with the thick-walled cells. These thin-walled cells present a thicker cuticle that is clearly visible in both SEM images and fluorescence pictures when the cuticle is isolated. In *Stangeria*, sclerified thick-walled pavement cells are as common as thin-walled cells in the adaxial epidermis (fig. 3*I*). In *Ceratozamia*, the abaxial epidermis also presents larger thick-walled cells, with wider lumina interspersed between the other pavement cells ("macrolumen cells"; fig. 3*F*).

Hypodermis. A continuous sclerified hypodermis on the adaxial side of the leaflets is present in *Dioon*, *Encephalartos*, *Macrozamia*, and *Lepidozamia* (figs. 2*A*, 3*A*, 3*C*–3*E*) as well as in some members of *Zamia*, such as *Z. meermanii* Calonje, *Z. pseudoparasitica* J.Yates, and *Z. furfuracea* L.f., while it is absent in *Ceratozamia*, *Stangeria*, *Bowenia*, *Microcycas*, *Macrozamia heteromera* C.Moore, and all the other species of *Zamia* for which data are available (fig. 3*B*, 3*F*–3*I*). The thickness of the adaxial hypodermis varies from one cell thick (as in *L. hopei* Regel, *E. manikensis* (Gilliland) Gilliland, and *Z. meermanii*) to several cells thick (as in *E. horridus* (Jacq.) Lehm.). On the abaxial side, a continuous or semicontinuous sclerified hypodermis in the intercostal regions is present in *Encephalartos*, *Lepidozamia*, and *Macrozamia* sect. *Macrozamia*.

Stomatal apparatus. The guard cells of all genera present an almost constant structure: the dorsal wall presents a substantial thickening in the medial section, and the cytoplasm is constricted to an oblique band toward the ventral side. Most of the cytoplasm of the guard cell is concentrated in the poles, which are distally raised with respect to the aperture (fig. 4*A*, 4*B*, 4*D*). Thin-walled subsidiary cells with ample vacuoles are present in all genera. These cells are adjacent to the guard cells on the dorsal side. Encircling cells (mostly thick walled) are usually placed distal to the subsidiary cells and form an anticlinally oriented pile (fig. 4*A*–4*C*). The number of encircling cells is variable within the same leaflet, with *Dioon* consistently having three layers; *Encephalartos* and *Macrozamia* having a variable number of one or two layers, with one layer being more common; and *Lepidozamia*, *Ceratozamia*, *Zamia*, *Microcycas*, and *Stangeria* having one layer. Both subsidiaries and encircling cells are arranged lateral to the guard cells. Polar cells of the stomatal apparatus tend to be slightly differentiated from normal pavement cells, and in some genera (*Dioon*, *Encephalartos*, *Ceratozamia*), they extend over the poles of the guard cells. Guard cells are sunken in a stomatal pit in all genera except for *Bowenia* and *Stangeria* (fig. 5*A*, 5*B*, 5*E*, 5*F*), where the guard cells are at the same level as the other pavement cells. In *Stangeria*, the encircling cells are not arranged distal to the subsidiaries, but they surround them laterally (fig. 5*C*, 5*D*). The stomatal apparatus of *Bowenia* lacks encircling cells (fig. 5*C*, 5*E*) but presents specialized subsidiary cells with lateral cuticular intrusion on the dorsal side.

Mesophyll. All species examined present a clear differentiation between an adaxial palisade and spongy parenchyma in the mesophyll, with the exception of the two species of *Bowenia*, where the mesophyll is composed of undifferentiated isodiametrical cells, and species of *Macrozamia* sect. *Parazamia*, where a slightly differentiated palisade-like layer is present both adaxially and abaxially and surrounds more or less undifferentiated parenchyma. Some species of *Encephalartos* and *Macrozamia* also present an abaxial palisade layer (fig. 3*E*). In *Dioon*, *Encephalartos*, *Lepidozamia*, and *Macrozamia* sect. *Macrozamia*, the palisade is composed of one layer of elongated cells (I-cells). In *Ceratozamia*, the palisade is composed of one layer of isodiametric cells with relatively thick walls. In *Zamia* and *Stangeria*, the palisade is composed of one or two layers of isodiametrical lobed cells (H-cells). Fibers are interspersed in the mesophyll of most species, being absent only in *E. humilis*, *Microcycas*, *Stangeria*, and some species of *Zamia*.

Mucilage canals. The distribution and morphology of mucilage canals present interesting variation at both the infra- and

Table 1

Characters Present in Different Species of Zamiaceae

	Adaxial sclerified hypodermis	Abaxial sclerified hypodermis	Adaxial girder sclerenchyma	Abaxial girder sclerenchyma	Mucilage canals in lamina	Palisade parenchyma	Fibers in mesophyll	Tranfusion tracheids in phloem pole
Bowenia serrulata	Absent	Absent	Absent	Absent	Absent	Undifferentiated	Present	Present
B. spectabilis	Absent	Absent	Absent	Absent	Absent	Undifferentiated	Present	Present
Ceratozamia alvarezii[a]	Absent	Absent	Absent	Absent	Multiple	One layer	Present	?
C. becerrae	Absent	Absent	Absent	Absent	Multiple	One layer	Present	?
C. brevifrons[a]	Absent	Absent	Absent	Absent	Multiple	One layer	Present	Present
C. chimalapensis[a]	Absent	Absent	Absent	Absent	Multiple	One layer	Present	Present
C. hildae	Absent	Absent	Absent	Absent	Multiple	One layer	Present	Present
C. mexicana	Absent	Absent	Absent	Absent	Multiple	One layer	Present	Present
C. mirandae[a]	Absent	Absent	Absent	Present	Multiple	One layer	Present	Present
C. norstogii	Discontinuous	Absent	Absent	Present	Multiple	One layer	Present	Present
C. robusta	Absent	Absent	Absent	Absent	Multiple	One layer	Present	Present
C. zoquorum	Absent	Absent	Absent	Present	Multiple	One layer	Present	?
Dioon angustifolium[a]	Present	Absent	Absent	Present	Associated with the bundle	One layer	Present	Present
D. argenteum[a]	Present	Absent	Absent	Present	Associated with the bundle	One layer	Present	Present
D. califanoi	Present	Absent	Absent	Present	Associated with the bundle	One layer	Present	Present
D. caputoi	Present	Absent	Absent	Present	Associated with the bundle	One layer	Present	Present
D. edule	Present	Absent	Absent	Present	Associated with the bundle	One layer	Present	Present
D. holmgrenii	Present	Absent	Absent	Present	Associated with the bundle	One layer	Present	Present
D. mejiae	Present	Absent	Absent	Present	Associated with the bundle	One layer	Present	Present
D. merolae	Present	Absent	Absent	Present	Associated with the bundle	One layer	Present	Present
D. purpusii	Present	Absent	Absent	Present	Associated with the bundle	One layer	Present	Present
D. rzedowskii	Present	Absent	Absent	Present	Associated with the bundle	One layer	Present	Present
D. sonorense[a]	Present	Absent	Absent	Present	Associated with the bundle	One layer	Present	Present
D. spinulosum	Present	Absent	Absent	Present	Associated with the bundle	One layer	Present	Present
D. stevensonii[a]	Present	Absent	Absent	Present	Associated with the bundle	One layer	Present	Present
D. tomasellii[a]	Present	Absent	Absent	Present	Associated with the bundle	One layer	Present	Present

Table 1 (*Continued*)

	Adaxial sclerified hypodermis	Abaxial sclerified hypodermis	Adaxial girder sclerenchyma	Abaxial girder sclerenchyma	Mucilage canals in lamina	Palisade parenchyma	Fibers in mesophyll	Tranfusion tracheids in phloem pole
Encephalartos altensteinii	Present	Present	Absent	Present	One large	One layer	Present	Present
E. caffer[a]	Present	Present	Absent	Present	One large	?	?	?
E. cupidus[a]	Present	Present	Absent	Present	One large	One layer	Absent	Present
E. cycadifolius[a]	Present	Present	Absent	Present	One large	One layer	Present	Present
E. eugenemaraisii[a]	Present	Present	Absent	Present	One large	One layer	Absent	Present
E. ferox	Present	Present	Absent	Present	One large	One layer	Present	Present
E. fridericiguilielmi[a]	Present	Present	Absent	Present	One large	One layer	Present	Present
E. ghellinckii[a]	Present	Present	Absent	Present	One large	One layer	Present	Present
E. heenanii[a]	Present	Present	Absent	Present	One large	One layer	Present	Present
E. horridus	Present	Present	Absent	Present	One large	One layer	Present	Present
E. humilis[a]	Present	Present	Absent	Present	Absent	One layer	Absent	Present
E. inopinus[a]	Present	Present	Absent	Present	One large	One layer	Present	Present
E. laevifolius[a]	Present	Present	Absent	Present	Absent	One layer	Present	Present
E. lanatus[a]	Present	Present	Absent	Present	Absent	One layer	Present	Present
E. latifrons[a]	Present	Present	Absent	Present	One large	One layer	Present	Present
E. laurentianus	Present	Present	Absent	Present	One large	One layer	Present	Present
E. lebomboensis[a]	Present	Present	Absent	Present	One large	?	?	?
E. lehmannii	Present	Present	Absent	Present	One large	One layer abaxial, one adaxial	Present	Present
E. longifolius[a]	Present	Present	Absent	Present	One large	?	?	?
E. macrostrobilus	Present	Present	Absent	Present	One large	One layer	Present	Present
E. manikensis	Present	Present	Absent	Present	One large	One layer	Present	Present
E. princeps[a]	Present	Present	Absent	Present	One large	One layer	Present	Present
E. trispinosus[a]	Present	Present	Absent	Present	One large	One layer	Present	Present
E. sclavoi	Present	Present	Absent	Present	One large	One layer	Present	Present
E. senticosus	Present	Present	Absent	Present	One large	One layer	Present	Present
E. transvenosus	Present	Present	Absent	Present	One large	One layer	Present	Present
E. umbeluziensis	Present	Present	Absent	Present	Absent	One layer	Present	Present
E. villosus	Present	Present	Absent	Present	Absent	One layer	Present	Present
Lepidozamia hopei	Present	Present	Absent	Present	One large	One layer	Present	Present
Macrozamia communis	Present	Present	Absent	Present	One large	One layer abaxial, one adaxial	Present	Present
M. heteromera	Absent	Absent	Absent	Absent	Absent	One layer abaxial, one adaxial	Present	Present
M. macdonnellii	Present	Present	Absent	Present	One large	One layer abaxial, one adaxial	Present	Present
M. moorei	Present	Present	Absent	Present	One large	One layer abaxial, one adaxial	Present	Present
M. pauli-guilielmi	Discontinuous	Absent	Absent	Present	Absent	One layer abaxial, one adaxial	Present	Present
Microcycas calocoma	Absent	Absent	Present	Present	Absent	Two layers, nonlobed	Absent	Absent
Stangeria eriopus	Absent	Absent	Present	Present	Absent	Two layers, lobed	Absent	Absent

Zamia acuminata[a]	Absent	Absent	Present	Present (collenchymatous)	Absent	Multiple layers, lobed	Present	?
Z. amplifolia	Absent	Absent	Present	Present	Absent	Two layers, lobed	Present	Absent
Z. angustifolia	Discontinuous	Absent	Present	Present	Absent	Two layers, lobed	Absent	Absent
Z. disodon	Absent	Absent	Present	Present (collenchymatous)	Absent	Two layers, lobed	Absent	Absent
Z. dressleri	Absent	Absent	Absent	Present (collenchymatous)	Absent	Two layers, lobed	Absent	Absent
Z. erosa	Discontinuous	Absent	Present	Present	Absent	Multiple layers, lobed	Absent	Absent
Z. gentryi	Absent	Absent	Present	Present (collenchymatous)	Absent	Two layers, lobed	Present	Absent
Z. hamannii	Absent	Absent	Absent	Present (collenchymatous)	Absent	Two layers, lobed	Present	Absent
Z. lindenii	Absent	Absent	Absent	Present (collenchymatous)	Absent	Two layers, lobed	Present	Absent
Z. loddigesii[a]	Absent	Absent	Present	Present	Absent	Two layers, lobed	Present	?
Z. meermanii	Present	Absent	Absent	Present	Absent	Multiple layers, lobed	Present	Absent
Z. nesophila	Absent	Absent	Absent	Present (collenchymatous)	Absent	Two layers, lobed	Present	Absent
Z. neurophyllidia	Absent	Absent	Absent	Present (collenchymatous)	Absent	Two layers, lobed	Present	Absent
Z. oligodonta	Absent	Absent	Present	Present	Absent	Two layers, lobed	Present	Absent
Z. portoricensis	Absent	Absent	Present	Present	Absent	Multiple layers, lobed	Absent	Absent
Z. pseudomonticola[a]	Absent	Absent	Present	Present	Absent	Multiple layers, lobed	Absent	?
Z. pseudoparasitica	Present	Absent	Absent	Present	Absent	Two layers, lobed	Present	Absent
Z. pumila[a]	Absent	Absent	Present	Present	Absent	?	?	?
Z. purpurea	Absent	Absent	Present	Present (collenchymatous)	Absent	Two layers, lobed	Absent	Absent
Z. pyrophylla	Present	Absent	Absent	Present	Absent	Two layers, lobed	Present	Absent
Z. roezlii	Absent	Absent	Present	Present (collenchymatous)	Absent	Two layers, lobed	Present	Absent
Z. skinneri	Absent	Absent	Absent	Present (collenchymatous)	Absent	Two layers, lobed	Present	Absent
Z. splendens[a]	Absent	Absent	Absent	Present (collenchymatous)	Absent	Two layers, lobed	?	?
Z. urep	Absent	Absent	Present	Present (collenchymatous)	Absent	Two layers, lobed	Present	Absent
Z. wallisii	Absent	Absent	Present	Present (collenchymatous)	Absent	Two layers, lobed	Present	Absent
Z. vazquezii	Absent	Absent	Absent	Absent	Absent	Two layers, lobed	Absent	Absent

Source. Lamb (1923); Koeleman et al. (1981); Acuña-Castillo and Marín-Méndez (2013); Pérez-Farrera et al. (2014, 2016); Magellan et al. (2018); Vovides et al. (2018).

[a] Scored from the literature.

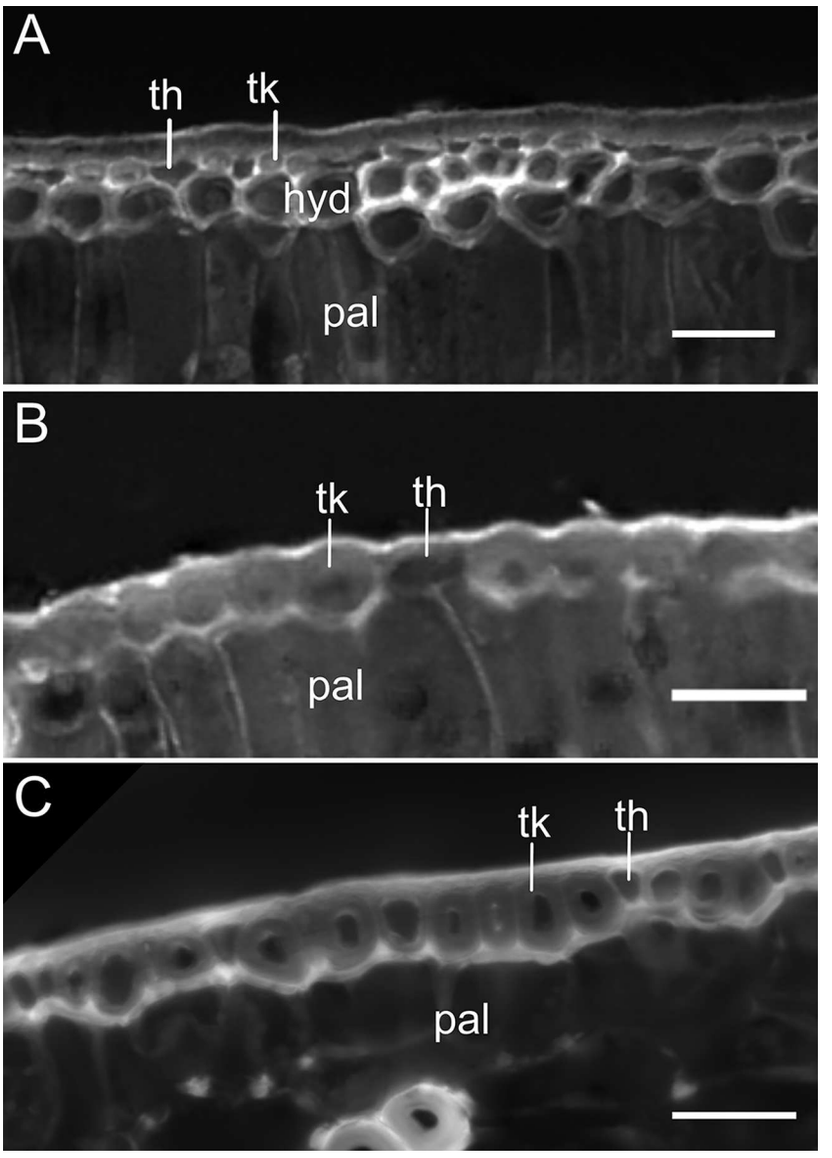

Fig. 2 Details of the adaxial epidermis, indicating the presence of two kinds of epidermal pavement cell. *A*, *Lepidozamia hopei*. *B*, *Microcycas calocoma*. *C*, *Ceratozamia mexicana*. hyd = hypodermis; pal = palisade parenchyma; th = thin-walled cells; tk = thick-walled cells. Scale bars = 50 μm.

suprageneric levels. Species of *Dioon* present large mucilage canals associated with the adaxial side of the vascular bundles (fig. 3*A*). Species of *Lepidozamia*, *Encephalartos* (with the exceptions of *E. villosus* Lem. and the closely related *E. umbeluziensis* R.A.Dyer, as well as *E. humilis* I.Verd., *E. laevifolius* Stapf & Burtt Davy, and *E. lanatus* Stapf & Burtt Davy), and *Macrozamia* sect. *Macrozamia* present a single large mucilage canal placed between the vascular bundles in a median to adaxial position. In *Bowenia*, the mucilage canals are present only in the contracted base of the leaflets and are placed adaxially but are not associated with the vascular bundles; the lamina part of the leaflets does not present mucilage canals. In *Ceratozamia*, small mucilage canals are present between the vascular bundles (fig. 6*A*, 6*B*); these are distributed more or less randomly in the spongy parenchyma. *Stangeria* presents mucilage canals in the midrib portion of the leaflet, distributed both adaxially and abaxially and interspersed in the ground tissue (fig. 6*C*, 6*D*); the lamina is, however, devoid of mucilage canals (fig. 3*I*). *Zamia*, *Microcycas*, and members of *Macrozamia* sect. *Parazamia* do not present any mucilage canals in the leaflets.

Vascular bundles. The vascular bundles are rather uniform in all genera, presenting exarch xylem and a bundle sheath with interspersed fibers. In *Stangeria*, some species of *Zamia*, and *Microcycas*, sclerified adaxial bundle sheath extensions (i.e., adaxial girder sclerenchyma) are present (fig. 3*G*–3*I*). In *Zamia*, this can be found in all *Zamia* from the Caribbean clade (sensu

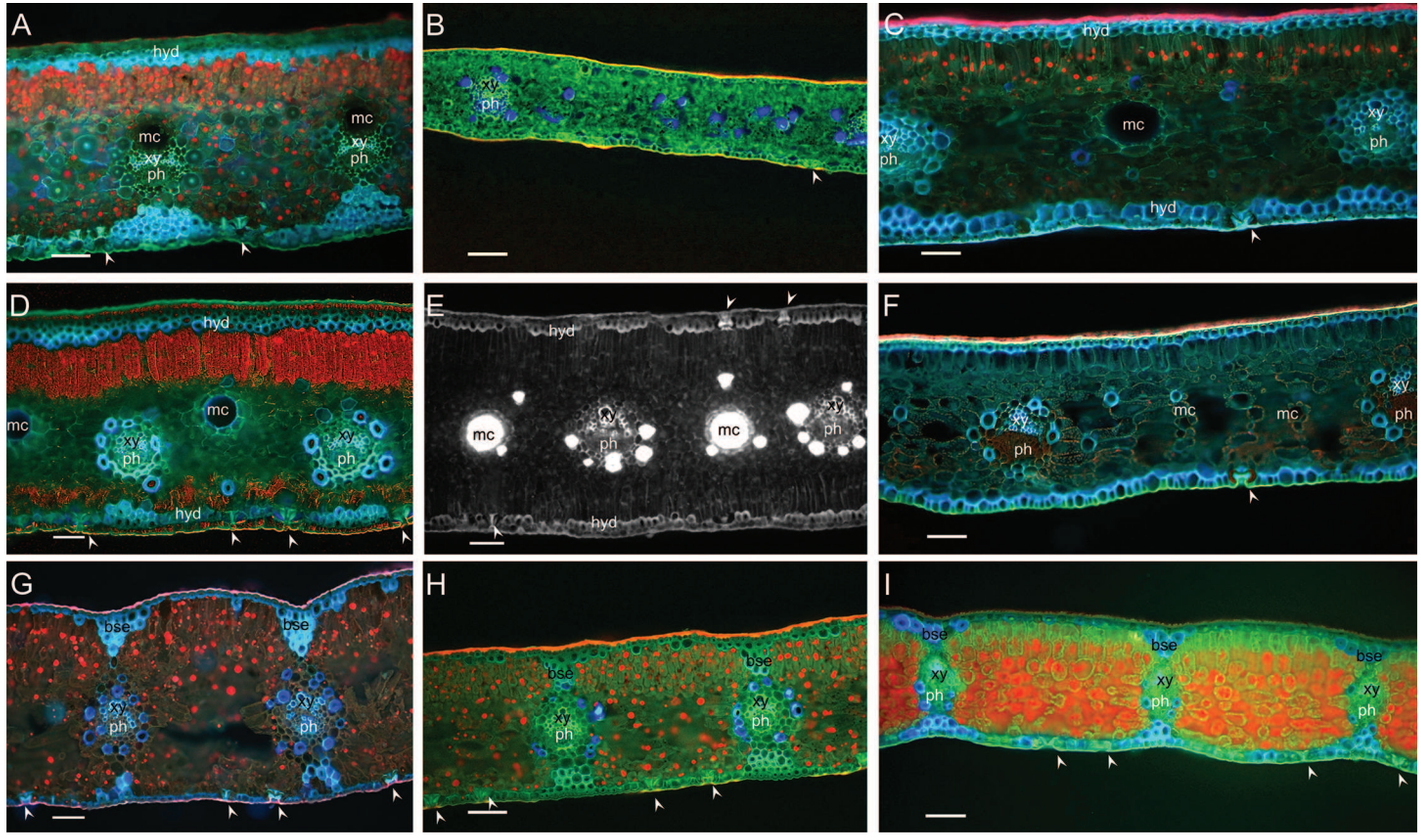

Fig. 3 Autofluorescence pictures illustrating the anatomy of the leaflets of representatives of all genera of the Zamiaceae. Sections are shown with adaxial side up. *A*, *Dioon rzedowskii*. *B*, *Bowenia serrulata*. *C*, *Lepidozamia hopei*. *D*, *Encephalartos horridus*. *E*, *Macrozamia moorei*. *F*, *Ceratozamia robusta*. *G*, *Microcycas calocoma*. *H*, *Zamia erosa*. *I*, *Stangeria eriopus*. bse = bundle sheath extension; hyd = sclerified hypodermis; mc = mucilage canal; ph = phloem; xy = xylem. Arrowheads indicate stomata. Scale bars = 100 μm.

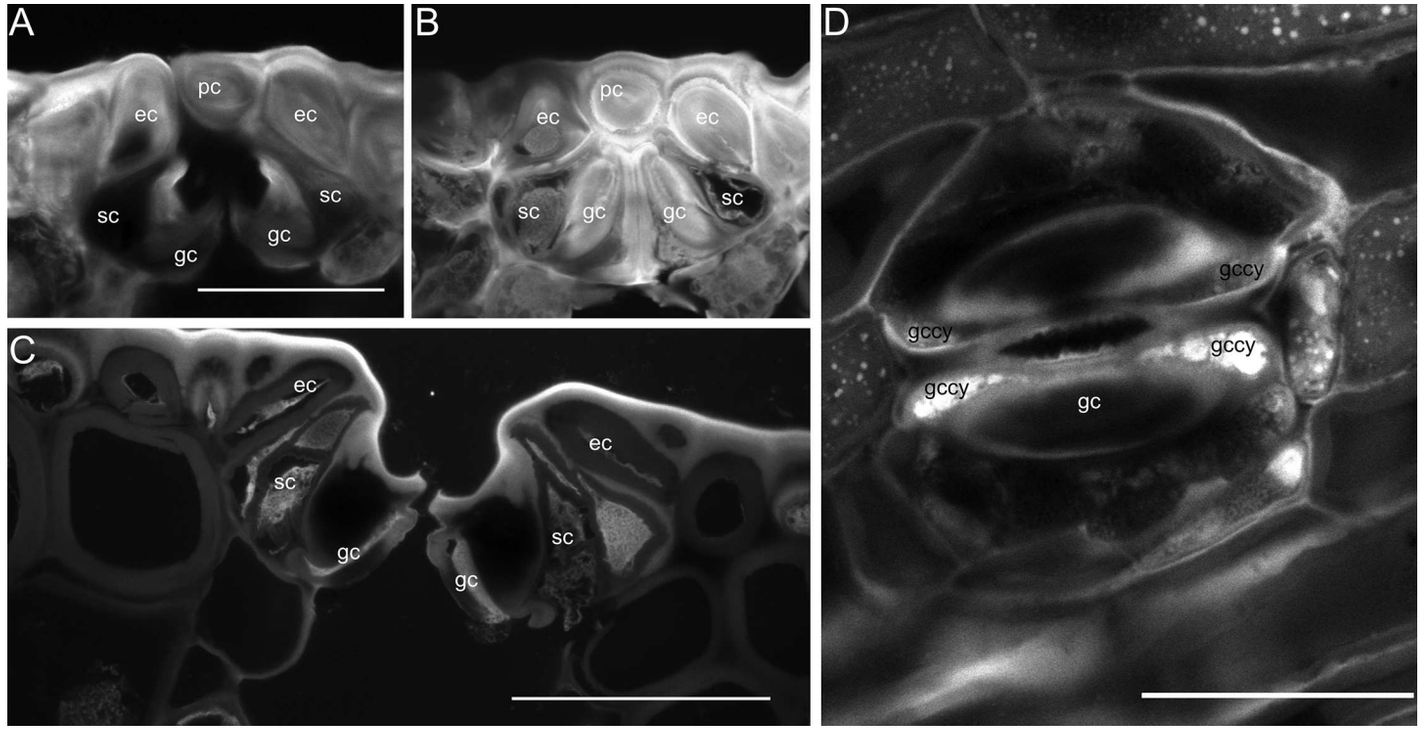

Fig. 4 Details of the stomatal apparatus of the Zamiaceae in section. *A*, *B*, *Macrozamia communis*. *C*, *D*, *Encephalartos villosus*. All three stomata shown present thin-celled, vacuolate subsidiary cells (sc) contacting the thick-walled guard cells (gc) and the encircling cells (ec). Thickened polar cells (pc) are visible in *A* and *B*. *D*, Paradermal sectioning shows the cytoplasm of the guard cells (gc) concentrated at the poles (gccy). *A*, *B*, and *D* represent optical slices from confocal stacks, with *A* and *B* coming from the same stomatal apparatus. *A* and *B* are shown at the same scale. Scale bars = 50 μm.

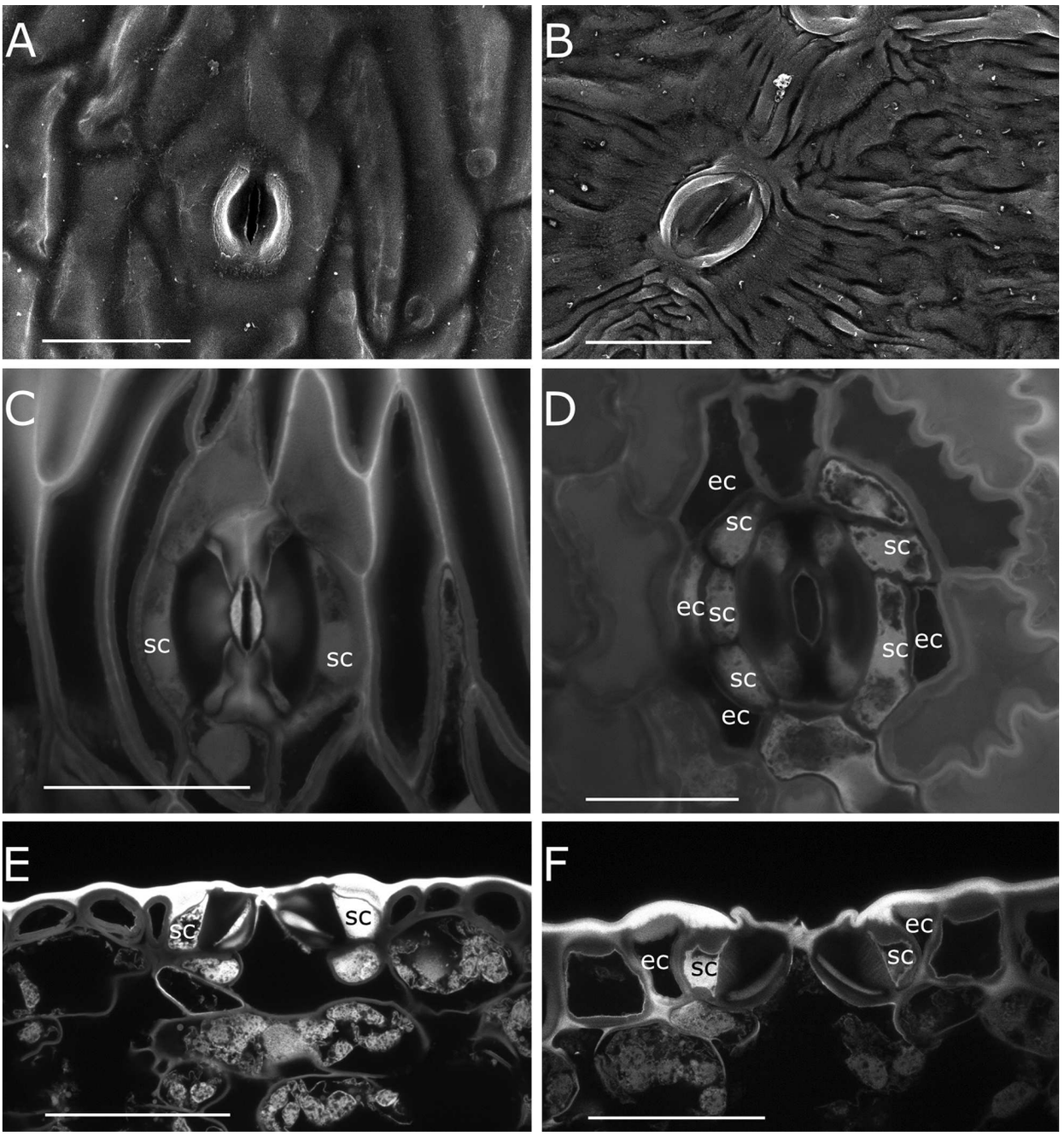

Fig. 5 Comparative illustrations of the stomatal apparatus of *Bowenia* and *Stangeria*. *A*, *C*, *E*, *Bowenia spectabilis*. *B*, *D*, *F*, *Stangeria eriopus*. *Bowenia* has monocyclic stomatal apparatuses with only subsidiary cells (sc), while *Stangeria* presents lateral encircling cells (ec). *A* and *B* are SEM images of outer leaf surfaces, while *C*, *D*, *E*, and *F* are confocal images of pseudo-Schiff propidium idodide–stained samples. Scale bars = 100 μm.

Calonje et al. 2019) as well as in species from the Mesoamerica and South America clade, but it seems to be absent from all species from the Isthmus clade, with the exclusion of the Acuminata clade. Abaxial girder sclerenchyma is present in all genera, with the exception of *Bowenia*. In *Ceratozamia*, it is present in only *C. norstogii* D.W.Stev., *C. zoquorum* Pérez-Farr., Vovides & Iglesias, and *C. mirandae* Vovides, Pérez-Farr. & Iglesias; is incipient in *C. mexicana* Brongn. (one layer); and is absent in the other species investigated. It is also absent in *Z. vazquezii* D.W.Stev., Sabato & De Luca. In some species of *Zamia*, especially those with plicate leaflets, the abaxial girder tissue is of a collenchymatous nature. Tissue interpretable as transfusion tissue is present around the bundles of all genera. In *Dioon*, *Encephalartos*, *Lepidozamia*, *Macrozamia*, *Bowenia*, and some

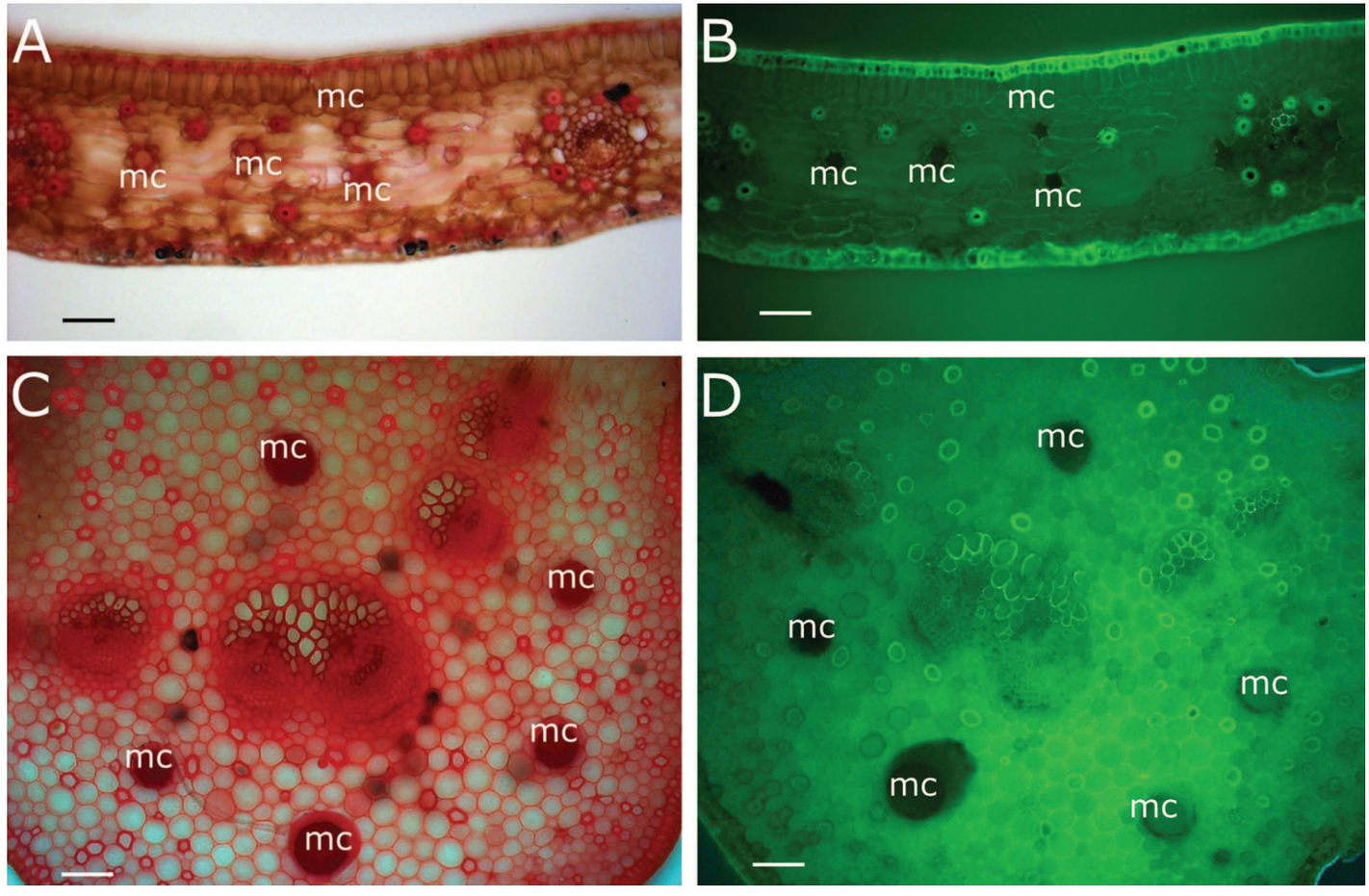

Fig. 6 Identification of mucilage canals illustrated using pseudo-Schiff propidium idodide–stained sections. *A* and *B* show the small mucilage canals (mc) in the lamina of *Ceratozamia robusta*; *C* and *D* show the canals scattered in the midrib of *Stangeria eriopus*. *A* and *C* are transmitted light images; *B* and *D* are fluorescent images. Scale bars = 100 μm.

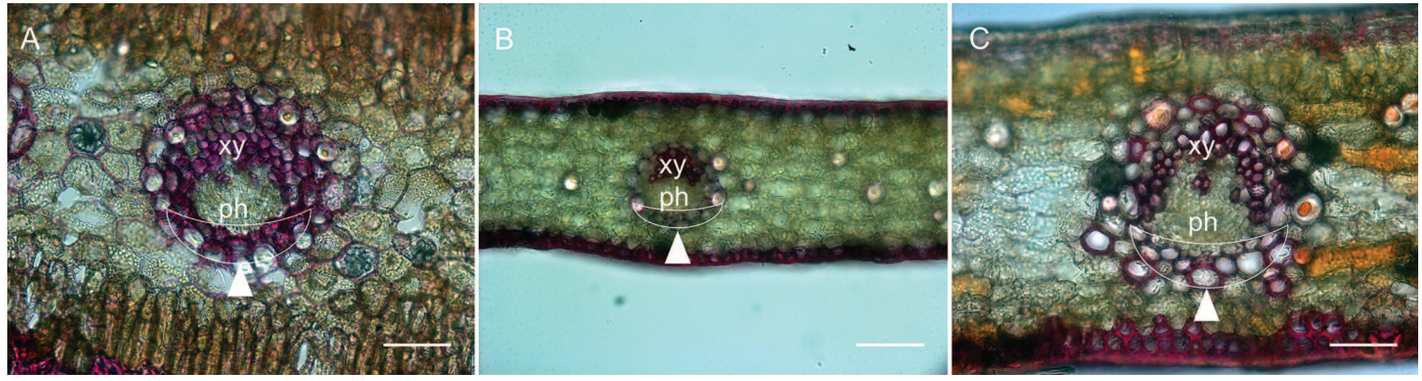

Fig. 7 Phloroglucinol-stained hand sections of leaflets illustrating the differentiation of the transfusion tissue associated with the vascular bundle at the phloem pole. *A*, *Macrozamia macdonnellii*. *B*, *Bowenia serrulata*. *C*, *Lepidozamia hopei*. Arrowheads indicate transfusion tracheids associated with the phloem pole of the vascular bundles. Transfusion tracheids are further highlighted by the dashed line. ph = phloem; xy = xylem. Scale bars = 100 μm.

species of *Ceratozamia*, this transfusion-like tissue is clearly differentiated, and tracheid-like cells are also present on the phloem pole of the bundles (fig. 7).

Phylogenetic Signal and Ancestral State Reconstruction

Both phylogenetic trees inferred are of comparable age, though with older splits compared with those of Condamine et al. (2015). Full trees are shown in figure S1 (figs. S1–S4 are available online).

All characters considered here present a strong phylogenetic signal on both topologies, as indicated both by the estimates of Pagel's λ (table 2) and by the parsimony-based shuffling test (table 3). Both the consistency index and the retention index indicate a low level of homoplasy, with the constrained tree explaining the evolution of the abaxial girder sclerenchyma, the fibers in the mesophyll, and the abaxial transfusion tissue better than the unconstrained tree (table 4). The character history reconstruction shows that most of the transitions happened at the internal nodes (fig. 8).

The evolutionary history of the adaxial hypodermis, the abaxial hypodermis, the abaxial girder sclerenchyma, the lobation of the parenchyma, the number of parenchyma layers, and the abaxial transfusion tissue is reconstructed consistently by the different methods and topology (figs. 8, S2–S4). The history of the adaxial girder sclerenchyma is reconstructed very differently by stochastic mapping and by parsimony, with the former reconstructing the presence of this character at all the stem nodes of the Zamiaceae (figs. 8, S2*B*), while the latter reconstructs its gain either somewhere at the base of the *Ceratozamia-Zamia* clade (unconstrained topology) or at the most recent common ancestor (MRCA) of *Stangeria* and *Zamia* (constrained topology). This is mostly due to the maximum-likelihood estimation of the Q-matrix for this character having a transition rate of 0 from absent to present; that is, the model does not allow for any gain of the character. The remaining characters are mostly consistent between methods, with only minor inconsistencies (fig. 8).

The ancestral node of the Zamiaceae and the MRCA of *Encephalartos* and *Zamia* are reconstructed as having the same character states, namely, the presence of an adaxial sclerified hypodermis, an abaxial girder sclerenchyma, fibers in the mesophyll, an abaxial transfusion tissue, an unlobed palisade with a single layer of cells, and a nonsclerified abaxial hypodermis. The other characters are reconstructed with a high degree of ambiguity, with the exception of the adaxial girder sclerenchyma, which is reconstructed as present by stochastic mapping and absent by parsimony (fig. 8*A*).

The origin of the Encephalarteae (*Macrozamia*, *Lepidozamia*, and *Encephalartos*) corresponds with the origin of an abaxial sclerified hypodermis and (but less clearly) a single mucilage canal between veins. An adaxial girder sclerenchyma was highly probably absent, while most other characters remained unchanged with respect to the parent node (fig. 8*B*). The MRCA of the *Ceratozamia-Zamia-Stangeria* clade underwent the loss of two characters: mucilage canals (though the condition is more uncertain with the assumption of primary homology between the multiple small canals of *Ceratozamia* and the single canals of the Encephalarteae) and the adaxial hypodermis. While stochastic mapping favors the retention of most ancestral states at this node, parsimony is more ambiguous (fig. 8*B*).

In the constrained topology, the *Stangeria-Zamia* clade is subtended by the gain of an adaxial girder sclerenchyma (according to parsimony) and the loss of fibers in the mesophyll (regained by a few clades within *Zamia*; fig. S4) and abaxial transfusion tissue (though the stochastic mapping is more ambiguous than parsimony). Whether the loss of mucilage canals in this clade is a genuine synapomorphy or an independent loss depends on both coding and method, with the stochastic mapping reconstruction of coding scheme 2 preferring the independent loss scenario (fig. 8*C*).

Table 2

Pagel's λ Values for the Characters Inferred Using the Two Different Topologies

	Unconstrained	Constrained
Adaxial sclerified hypodermis	.972	.969
Abaxial sclerified hypodermis	1.000	.99
Adaxial girder sclerenchyma	.942	.821
Abaxial girder sclerenchyma	1.000	1.000
Mucilage canals (coding 1)	.972	.978
Mucilage canals (coding 2)	.948	.96
Palisade lobation	1.000	1.000
Palisade layer no.	1.000	.987
Fibers in mesophyll	.749	.89
Tracheid-like transfusion tissue	1.000	1.000

Table 3

Results of the Parsimony Randomization Test for Each Character on the Two Different Topologies

Tree, character	*P* value	Steps observed	Steps expected
Unconstrained:			
Adaxial sclerified hypodermis	<.001	2	20 (14–26)
Abaxial sclerified hypodermis	<.001	2	21 (13–27)
Adaxial girder sclerenchyma	<.001	5	10 (7–11)
Abaxial girder sclerenchyma	<.001	4	9 (6–9)
Mucilage canals (coding 1)	<.001	8	29 (23–35)
Mucilage canals (coding 2)	<.001	8	25 (19–31)
Palisade lobation	<.001	3	16 (12–18)
Palisade layer no.	<.001	6	18 (13–19)
Fibers in mesophyll	.015	7	10 (6–10)
Abaxial transfusion tissue	<.001	2	11 (7–12)
Constrained:			
Adaxial sclerified hypodermis	<.001	2	21 (13–25)
Abaxial sclerified hypodermis	<.001	2	21 (14–26)
Adaxial girder sclerenchyma	<.001	5	11 (7–11)
Abaxial girder sclerenchyma	<.001	4	9 (5–9)
Mucilage canals (coding 1)	<.001	8	29 (23–35)
Mucilage canals (coding 2)	<.001	8	25 (19–31)
Palisade lobation	<.001	3	16 (11–18)
Palisade layer no.	<.001	6	18 (14–19)
Fibers in the mesophyll	.001	6	10 (6–10)
Abaxial transfusion tissue	<.001	1	11 (7–12)

Discussion

Our results indicate that leaflet anatomy presents a degree of variation in the Zamiaceae. All genera present a rather uniform leaflet anatomy, in agreement with previous studies (Barone

Table 4

Consistency Index and Retention Index for All Characters over the Two Different Topologies

	Unconstrained consistency index	Retention index	Constrained consistency index	Retention index
Adaxial sclerified hypodermis	.5	.96	.5	.96
Abaxial sclerified hypodermis	.5	.96	.5	.96
Adaxial girder sclerenchyma	.2	.6	.2	.6
Abaxial girder sclerenchyma	.25	.62	.33	.75
Mucilage canals (coding 1)	.37	.85	.37	.85
Mucilage canals (coding 2)	.25	.8	.25	.8
Palisade lobation	.67	.94	.67	.94
Palisade layer no.	.5	.81	.5	.81
Fibers in mesophyll	.14	.33	.17	.44
Abaxial transfusion tissue	.5	.91	1	1

Lumaga et al. 2015; Magellan et al. 2018; Vovides et al. 2018). However, the genera *Zamia*, *Encephalartos*, and *Macrozamia* present a higher degree of variation, with the first presenting the highest variability.

Unfortunately, given the radically different architecture of the leaflets of *Cycas*, it is hard to identify homologies between the characters identified here and the ones described for that genus (Griffith et al. 2014). The presence of both thin- and thick-walled epidermal cells seems to represent a genuine synapomorphy of the Zamiaceae as a whole, as previously suggested on the basis of cuticular evidence (Coiro and Pott 2017). Some of the characters of the mesophyll of *Cycas*, such as the absence of both an adaxial and an abaxial sclerified hypodermis, could be homologous to the conditions present in some genera of the Zamiaceae. However, the different structure of the cycadacean leaflet, with its midrib acting as the main source of structural support, could also explain the absence of such structural tissue in the lamina.

Congruence between leaflet anatomy and molecular phylogenies. Some of the characters identified in this study are variable among genera and present some potential for delimiting subfamilial clades. The members of the tribe Encephalarteae sensu Stevenson (1992; i.e., *Encephalartos*, *Macrozamia*, and *Lepidozamia*) share some potentially synapomorphic characters, such as the presence of large mucilage canals in the areas between the vascular bundles and the presence of an adaxial sclerified hypodermis. These are reconstructed as ancestral in the clade by both parsimony and stochastic mapping approaches on both topologies (fig. 8*A*). Moreover, only among members of this clade is it possible to find fully bifacial leaflets with an adaxial palisade parenchyma and adaxial stomata. These are quite common in *Macrozamia* sect. *Macrozamia* (*M. moorei* F.Muell., *M. macdonnellii* (F.Muell. ex Miq.) A.DC., *M. riedlei* (Gaudich.) C.A.Gardner, etc.). The main deviation from the "bauplan" of the Encephalarteae is present in the members of *Macrozamia* sect. *Parazamia*: these species lack clear mucilage canals in the lamina as well as a continuous hypodermis, and their mesophyll lacks differentiation between the palisade and the spongy parenchyma (Johnson 1959; Carpenter 1991). These species are thought to be neotenous derivatives (Carpenter 1991), and the derived condition of their leaflets is supported by our analyses (figs. S2–S4). Within the Encephalarteae, the genus *Lepidozamia* and some members of *Encephalartos* are extremely hard to distinguish on the basis of their leaflet anatomy; both have a single-layered hypodermis, short palisade cells, few fibers between the bundles, and relatively shallow guard cells. This supports the close relationship between these two genera suggested by molecular phylogenies.

Our investigation also supports the separation of *Dioon* and the Encephalarteae. The leaflet characters that are shared by these two groups (presence of an adaxial sclerified hypodermis, adaxial girder sclerenchyma, fibers in the mesophyll, and adaxial transfusion tissue) are reconstructed as plesiomorphic for the Zamiaceae as a whole. On the other hand, the presence of mucilage canals associated with the bundles, nonlignified fibers (Magellan et al. 2018), and three layers of encircling cells in their stomatal apparatuses (Barone Lumaga et al. 2015; Vovides et al. 2018) clearly sets *Dioon* apart from the other genera, consistent with its isolated phylogenetic placement and its long independent history (Condamine et al. 2015).

Leaflet anatomy supports a close relationship between Stangeria *and* Zamia-Microcycas. Leaflet anatomy also shows unexpected similarities in *Zamia*, *Microcycas*, and the morphologically diverging *Stangeria*. These three genera share the presence of both abaxial and adaxial girder sclerenchyma (even if the latter is variable within *Zamia*), the absence of mucilage canals in the leaflet lamina, abaxial transfusion tissue, and fibers in the mesophyll (present in some species of *Zamia*). Moreover, *Stangeria* and *Zamia* share the presence of lobed H-type palisade parenchyma, while *Microcycas* presents an I-type palisade. Given the uncertainty in the placement of *Stangeria* and the old age of the split between the genera in this group, the history of trait evolution is more ambiguous than in the Encephalarteae, with methods and topologies giving different answers (fig. 8*B*, 8*C*). However, the constrained topology with *Stangeria* as sister to *Microcycas* and *Zamia* seems to better explain the evolution of leaflet characters than the unconstrained topology with *Stangeria* as sister to *Ceratozamia* (table 4). Our results suggest that a reinvestigation of other anatomical aspects of *Stangeria* might still reveal characters validating its placement within Zamiaceae.

Surprisingly, *Ceratozamia* seems to share very few anatomical characters with *Zamia*, *Microcycas*, and *Stangeria*. This runs contrary to the results obtained using general leaf morphology, with *Ceratozamia* sharing articulated leaflets and the presence of stipules with *Zamia* and *Microcycas* (but not *Stangeria*, where leaflets are decurrent and the base of the leaves is surrounded by

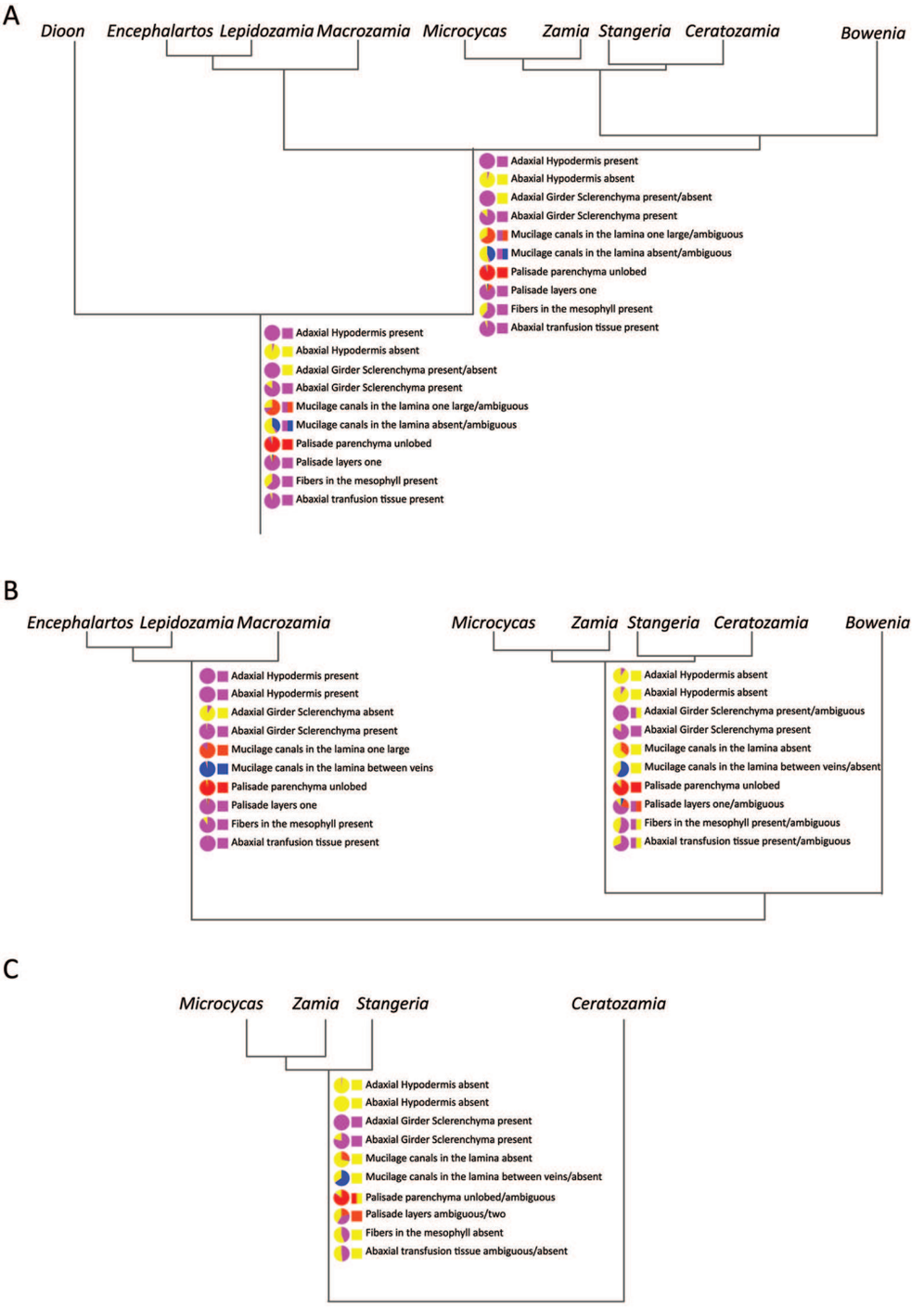

Fig. 8 Summary of the ancestral state reconstruction analyses of the ancestral nodes of the Zamiaceae (*A*), the ancestral node of Encephalarteae and the *Ceratozamia-Zamia-Stangeria* clade (*B*), and the *Stangeria-Zamia* clade (*C*). Circles represent results of the stochastic mapping analysis, while squares represent parsimony reconstruction on the unconstrained tree (*A*, *B*) or the constrained tree (*C*). For characters 1–4, 9, and 10, cyan represents present, and yellow represents absent; for character 5, red represents one large, blue represents multiple, cyan represents associated with veins, and yellow represents absent; for character 6, blue represents between veins, cyan represents associated with veins, and yellow represents absent; for character 7, red represents unlobed, yellow represents lobed, and cyan represents undifferentiated; and for character 8, blue represents zero, cyan represents one, red represents two, and yellow represents multiple.

a cowl-like structure interpreted as vascularized stipules). However, it would be coherent with a long independent history of *Ceratozamia* as retrieved by molecular dating analyses (Salas-Leiva et al. 2013; Condamine et al. 2015).

Leaflet anatomy does not support Stangeriaceae. Our reinvestigation identifies some shared characters for *Bowenia* and *Stangeria*, that is, the absence of mucilage canals in the lamina and the presence of stomata with guard cells at the same level as the epidermal pavement cells ("flush" guard cells). The latter character state separates these two genera from all other genera of the Cycadales, which present stomata that are more or less sunken with respect to the epidermis (fig. 4). It is also quite rare in fossil leaves assigned to the Cycadales, being limited to *Eobowenia* (*Almargemia*) *incrassata* M.Coiro & C.Pott and *Mesodescolea plicata* S.Archang. from the Early Cretaceous of Argentina. The former has been hypothesized to be a stem relative of *Bowenia* (Coiro and Pott 2017), and the latter has been linked by its authors with *Stangeria* (Archangelsky 1963; Archangelsky and Petriella 1971; Artabe and Archangelsky 1992). Coiro and Pott (2017) suggested on the basis of cuticular anatomy that the stomatal apparatus in *Bowenia* was monocyclic; that is, it lacked encircling cells, while the stomatal apparatus of *Stangeria*, in being dicyclic, more closely resembled that found in other cycads. Our observations confirm this inference, clearly showing that the stomatal apparatuses of *Bowenia* and *Stangeria* are constructed in a radically different way (fig. 5*C*–5*F*). Another stomatal character that was thought to link *Stangeria* and *Bowenia* as well as *Mesodescolea* was the presence of "circular" stomata. However, our investigation reveals that the morphology of the guard cells in *Stangeria* and *Bowenia* conforms to the elongated morphology of all other members of the Cycadales (fig. 5*C*, 5*D*) and cannot really be homologized with the "circular" stomata present in many angiosperms or ferns. Besides the stomatal apparatus, the leaflets of *Bowenia* and *Stangeria* are extremely divergent. *Bowenia* presents leaflets with an undifferentiated mesophyll of densely packed parenchyma cells and fibers, while *Stangeria* has a clearly differentiated palisade and spongy parenchyma without fibers. Moreover, the bundles in *Stangeria* are associated with bundle sheath extensions, while in *Bowenia*, the bundles are free, and neither adaxial nor abaxial girder sclerenchyma is present. Such divergence in leaflet anatomy seems to be in stark contrast to the characters identified from morphological and anatomical studies of the whole plants, with many synapomorphies identified for the Stangeriaceae (Stevenson 1992). However, if some of these characters, such as the presence of root buds and vascularized stipules, are harder to interpret as independent gains, others are more easily explained as parallelisms or convergence. For example, the absence of an omega pattern in the rachis, which has recently been connected to the hydraulic need of a simple pinnate leaf (Tomlinson et al. 2018), is expected given the different functional needs of a bipinnate leaf (such as in *Bowenia*) and a leaf with multiple-veined midribs (such as in *Stangeria*). A reevaluation of these characters, perhaps in a developmental framework, could help to disentangle the selective or developmental causes of these striking apparent convergences.

Paeodomorphic shifts and convergence. Some characters shared by *Bowenia*, *Ceratozamia*, and *Macrozamia* sect. *Parazamia*, such as the lack of mucilage canals in the lamina, the lack of abaxial girder sclerenchyma, and the absence of a sclerified hypodermis, are mainly related to reduction. In *Macrozamia* sect. *Parazamia*, these losses were probably a result of neoteny (Johnson 1959; Carpenter 1991). Recently, paedomorphosis has been suggested as an important mechanism acting in the evolution of *Ceratozamia* (Medina-Villarreal et al. 2019). In the case of *Bowenia*, a paedomorphic origin could also explain some of the other peculiar traits of this genus, such as the production of a single leaf per growing season, the irregular production of cataphylls, and the subterranean tuberous habit. Progenesis (i.e., an early onset of mature characteristics during development) seems to fit the pattern of wood development in *Bowenia* better than neoteny, given that *Bowenia* completely lacks the scalariform tracheids that characterize the xylem of juvenile cycads (Chrysler 1937). However, the absence of close living relatives and the old divergence of *Bowenia* from the other Zamiaceae (Coiro and Pott 2017) make testing this hypothesis rather difficult. The small size of the leaflets in the close relative *Eobowenia* might represent another indication of progenetic reduction, but a more detailed understanding of the morphology of other fossil relatives as well as a deeper understanding of the development of extant *Bowenia* is required to solve this puzzle.

Acknowledgments

M. Coiro thanks H. Peter Linder for his support of this work. The visit of M. Coiro to the Montgomery Botanical Center was partially supported by the Kelly Foundation. Confocal imaging was performed with equipment maintained by the Centre for Microscopy and Image Analysis, University of Zurich. We thank two anonymous reviewers for comments that vastly improved the manuscript.

Literature Cited

Acuña-Castillo R, W Marín-Méndez 2013 Comparative anatomy of leaflets of *Zamia acuminata* and *Z. pseudomonticola* (Zamiaceae) in Costa Rica. Rev Biol Trop 61:539–546.

Alvin KL, MC Boulter 1974 A controlled method of comparative study for Taxodiaceous leaf cuticles. Bot J Linn Soc 69:277–286.

Archangelsky S 1963 A new Mesozoic flora from Ticó, Santa Cruz Province, Argentina. Bull Br Mus Nat Hist Geol 8:45–92.

Archangelsky S, B Petriella 1971 Notas sobre la flora fósil de la zona de Ticó, Provincia de Santa Cruz. IX. Nuevos datos acerca de la morfología foliar de Mesodescolea plicata Arch. (Cycadales, Stangeriaceae). Bol Soc Argent Bot 14:88–94.

Artabe A, S Archangelsky 1992 Las Cycadales *Mesodescolea* Archangelsky emend. Archangelsky y Petriella 1971 (Cretácico) y *Stangeria* Moore (Actual). Ameghiniana 29:115–123.

Barone Lumaga MR, M Coiro, E Truernit, B Erdei, P De Luca 2015 Epidermal micromorphology in *Dioon*: did volcanism constrain *Dioon* evolution? Bot J Linn Soc 179:236–254.

Bollback JP 2006 SIMMAP: stochastic character mapping of discrete traits on phylogenies. BMC Bioinformat 7:88.

Bouckaert RR, AJ Drummond 2017 bModelTest: Bayesian phylogenetic site model averaging and model comparison. BMC Evol Biol 17:42.

Brenner ED, DW Stevenson, RW Twigg 2003 Cycads: evolutionary innovations and the role of plant-derived neurotoxins. Trends Plant Sci 8:446–452.

Bush SE, JD Weckstein, DR Gustafsson, J Allen, E DiBlasi, SM Shreve, R Boldt, HR Skeen, KP Johnson 2016 Unlocking the black box of feather louse diversity: a molecular phylogeny of the hyper-diverse genus *Brueelia*. Mol Phylogenet Evol 94:737–751.

Calonje M, AW Meerow, MP Griffith, D Salas-Leiva, AP Vovides, M Coiro, J Francisco-Ortega 2019 A time-calibrated species tree phylogeny of the New World cycad genus *Zamia* L. Int J Plant Sci 180:286–314.

Carpenter R 1991 *Macrozamia* from the early Tertiary of Tasmania and a study of the cuticles of extant species. Aust Syst Bot 4:433–444.

Christenhusz MJM, JL Reveal, A Farjon, MF Gardner, RR Mill, MW Chase 2011 A new classification and linear sequence of extant gymnosperms. Phytotaxa 19:55–70.

Chrysler M 1937 Persistent juveniles among the cycads. Bot Gaz 98:696–710.

Clugston JAR, MP Griffith, GJ Kenicer, CE Husby 2016 *Zamia* (Zamiaceae) phenology in a phylogenetic context: does in situ reproductive timing correlate with ancestry? Edinb J Bot 73:345–370.

Coiro M, G Chomicki, JA Doyle 2018 Experimental signal dissection and method sensitivity analyses reaffirm the potential of fossils and morphology in the resolution of the relationship of angiosperms and Gnetales. Paleobiology 44:490–510.

Coiro M, C Pott 2017 *Eobowenia* gen. nov. from the Early Cretaceous of Patagonia: indication for an early divergence of *Bowenia*? BMC Evol Biol 17:97.

Coiro M, E Truernit 2017 Xylem characterization using improved pseudo-Schiff propidium iodide staining of whole mount samples and confocal laser-scanning microscopy. Pages 127–132 *in* M de Lucas, P Etchhells, eds. Xylem. Humana, New York.

Condamine FL, NS Nagalingum, CR Marshall, H Morlon 2015 Origin and diversification of living cycads: a cautionary tale on the impact of the branching process prior in Bayesian molecular dating. BMC Evol Biol 15:65.

Drummond AJ, A Rambaut 2007 BEAST: Bayesian evolutionary analysis by sampling trees. BMC Evol Biol 7:214.

Erdei B, M Calonje, A Hendy, N Espinosa 2018 A review of the Cenozoic fossil record of the genus *Zamia* L. (Zamiaceae, Cycadales) with recognition of a new species from the late Eocene of Panama: evolution and biogeographic inferences. Bull Geosci 93:185–204.

Fenster CB, WS Armbruster, P Wilson, MR Dudash, JD Thomson 2004 Pollination syndromes and floral specialization. Annu Rev Ecol Evol Syst 35:375–403.

Florin R 1933 Studien über die Cycadales des Mesozoikums, nebst Erörterungen über die Spaltöffnungsapparate der bennettitales. Almqvist & Wiksells Boktryckeri, Stockholm.

Gao Z, BA Thomas 1989 A review of fossil cycad megasporophylls, with new evidence of *Crossozamia* Pomel and its associated leaves from the lower Permian of Taiyuan, China. Rev Palaeobot Palynol 60:205–223.

Greguss P 1968 Xylotomy of the living cycads, with a description of their leaves and epidermis. Akademiai Kiado, Budapest.

Griffith MP, TM Magellan, PB Tomlinson 2014 Variation in leaflet structure in *Cycas* (Cycadales: Cycadaceae): does anatomy follow phylogeny and geography? Int J Plant Sci 175:241–255.

Gutiérrez-Ortega JS, T Yamamoto, AP Vovides, MA Pérez-Farrera, JF Martínez, F Molina-Freaner, Y Watano, T Kajita 2018 Aridification as a driver of biodiversity: a case study for the cycad genus *Dioon* (Zamiaceae). Ann Bot 121:47–60.

Harmon LJ, JT Weir, CD Brock, RE Glor, W Challenger 2008 GEIGER: investigating evolutionary radiations. Bioinformatics 24:129–131.

Harris T 1961 The fossil cycads. Palaeontology 4:313–323.

Hill RS 1978 Two new species of *Bowenia* Hook, ex Hook, f. from the Eocene of eastern Australia. Aust J Bot 26:837–846.

——— 1980 Three new Eocene cycads from eastern Australia. Aust J Bot 28:105.

Johnson LAS 1959 The families of cycads and the Zamiaceae of Australia. Proc Linn Soc N S W 84:64–117.

Koeleman A, PJ Robbertse, A Eicker 1981 Die anatomie van die pinnas van die Suid-Afrikaanse spesies van *Encephalartos* Lehm. S Afr J Bot 47:247–271.

Lamb MA 1923 Leaflets of Cycadaceae. Bot Gaz 76:185–202.

Lindstrom AJ 2009 Typification of some species names in *Zamia* L. (*Zamiaceae*), with an assessment of the status of *Chigua* D. Stev. Taxon 58:265–270.

Maddison WP, D Maddison 2005 Mesquite: a modular system for evolutionary analysis. Evolution 62:1103–1118.

Maddison WP, M Slatkin 1991 Null models for the number of evolutionary steps in a character on a phylogenetic tree. Evolution 45:1184–1197.

Magellan TM, MP Griffith, A Ricciardi, BA Huggett, PB Tomlinson 2018 A novel type of fiber in the leaves of the cycad *Dioon*. Int J Plant Sci 179:231–240.

Medina-Villarreal A, J González-Astorga, AE de los Monteros 2019 Evolution of *Ceratozamia* cycads: a proximate-ultimate approach. Mol Phylogenet Evol 139:106530.

Miller MA, W Pfeiffer, T Schwartz 2010 Creating the CIPRES Science Gateway for inference of large phylogenetic trees. 2010 Gateway Computing Environments Workshop, New Orleans, November 14.

Nagalingum NS, CR Marshall, TB Quental, HS Rai, DP Little, S Mathews 2011 Recent synchronous radiation of a living fossil. Science 334:796–799.

Pérez-Farrera MA, AP Vovides, S Avendaño 2014 Morphology and leaflet anatomy of the *Ceratozamia norstogii* (Zamiaceae, Cycadales) species complex in Mexico with comments on relationships and speciation. Int J Plant Sci 175:110–121.

Pérez-Farrera MA, AP Vovides, C Ruiz-Castillejos, S Galicia, A Cibrián-Jaramillo, S López 2016 Anatomy and morphology suggest a hybrid origin of *Zamia katzeriana* (Zamiaceae). Phytotaxa 270:161–181.

Rai HS, HE O'Brien, PA Reeves, RG Olmstead, SW Graham 2003 Inference of higher-order relationships in the cycads from a large chloroplast data set. Mol Phylogenet Evol 29:350–359.

Rambaut A, AJ Drummond, D Xie, G Baele, MA Suchard 2018 Posterior summarisation in Bayesian phylogenetics using Tracer 1.7. Syst Biol 67:901–904.

Revell LJ 2012 phytools: an R package for phylogenetic comparative biology (and other things). Methods Ecol Evol 3:217–223.

Salas-Leiva DE, AW Meerow, M Calonje, MP Griffith, J Francisco-Ortega, K Nakamura, DW Stevenson, CE Lewis, S Namoff 2013 Phylogeny of the cycads based on multiple single-copy nuclear genes: congruence of concatenated parsimony, likelihood and species tree inference methods. Ann Bot 112:1263–1278.

Schindelin J, I Arganda-Carreras, E Frise, V Kaynig, M Longair, T Pietzsch, S Preibisch, et al 2012 Fiji: an open-source platform for biological-image analysis. Nat Methods 9:676.

Stevenson DW 1981 Observations on ptyxis, phenology, and trichomes in the Cycadales and their systematic implications. Am J Bot 68:1104–1114.

——— 1990 Morphology and systematics of the Cycadales. Mem NY Bot Gard 57:8–55.

——— 1992 A formal classification of the extant cycads. Brittonia 44:220–223.

Stevenson DW, K Norstog, D Molsen 1996 Midribs of cycad pinnae. Brittonia 48:67–74.

Suchard MA, A Rambaut 2009 Many-core algorithms for statistical phylogenetics. Bioinformatics 25:1370–1376.

Thomas HH, N Bancroft 1913 VI. On the cuticles of some recent and fossil cycadean fronds. Bot J Linn Soc 8:155–204.

Tomlinson PB, A Ricciardi, BA Huggett 2018 Cracking the omega code: hydraulic architecture of the cycad leaf axis. Ann Bot 121:483–488.

Vovides AP, JAR Clugston, JS Gutiérrez-Ortega, MA Pérez-Farrera, MY Sánchez-Tinoco, S Galicia 2018 Epidermal morphology and leaflet anatomy of *Dioon* (Zamiaceae) with comments on climate and environment. Flora 239:20–44.

Wilf P, DW Stevenson, NR Cúneo 2016 The last Patagonian cycad, *Austrozamia stockeyi* gen. et sp. nov., early Eocene of Laguna del Hunco, Chubut, Argentina. Botany 94:817–829.

Wright IJ, PB Reich, M Westoby, DD Ackerly, Z Baruch, F Bongers, J Cavender-Bares, et al 2004 The worldwide leaf economics spectrum. Nature 428:821–827.

Zgurski JM, HS Rai, QM Fai, DJ Bogler, J Francisco-Ortega, SW Graham 2008 How well do we understand the overall backbone of cycad phylogeny? new insights from a large, multigene plastid data set. Mol Phylogenet Evol 47:1232–1237.